

EDDY-RESOLVING REYNOLDS-STRESS MODELLING OF THERMAL STRIPING IN A MIXING TEE

Ivan Joksimovic^{1,*}, Suad Jakirlic¹

¹Institute of Fluid Mechanics and Aerodynamics, Technical University Darmstadt, Germany

ABSTRACT

An eddy-resolving simulation method utilizing a full Second-Moment Closure model to describe the dynamics of residual turbulence was employed to reproduce the phenomena of thermal striping in a T-Junction confinement. The high Reynolds number WATLON water experiment [1] has been selected as the reference configuration. Use of this novel turbulence model enables the correct capturing of the underlying fluctuating flow and thermal fields and associated frequency content under conditions of appropriately coarsened spatial resolution. Very good agreement was obtained between the computational results and the measurements, both in terms of the first- and second-order statistics.

1 INTRODUCTION AND MOTIVATION

Flow configurations relevant to NPP (Nuclear Power Plant) piping systems are often classified as high Reynolds number flows which exhibit complex features like secondary motion, separation-, recirculation- and re-attachment zones, etc. In the case of a non-isothermal flow, temporal dynamics of temperature field is of decisive importance in relation to development of fatigue-related phenomena in the solid structure confining the flow. Conventional, inherently-steady RANS (Reynolds-Averaged Navier-Stokes) turbulence models are, despite obvious advantage in regard to computational effort, incapable to satisfactorily reproduce such flow details. On the other hand, the use of an LES (Large-Eddy Simulation) methodology has strict meshing requirements that result in high computational penalties, making them non-preferable choice for industrial use. In this paper, we attempt to circumvent the aforementioned difficulty by applying a RANS-based eddy-resolving methodology to reproduce correctly industrially relevant phenomena of thermal striping in the T-junction-shaped pipe configuration. Experimental setup serving as a validation basis represents a water experiment WATLON, reported in [1]. In this experiment, two fluid streams with different temperatures mix in a T-Junction confinement, which consists of two perpendicularly positioned pipe-lines. The stream coming from the main horizontal pipe carries the hot fluid, whereas a perpendicularly injected branch stream carries a colder fluid. By varying the mass flow rate in the main stream, flow configurations are created exhibiting strong topological differences. The configuration denoted as 'wall-jet' is considered presently as experimental reference. Geometrical parameters and boundary conditions which are used in the experiment are listed in Table 1.

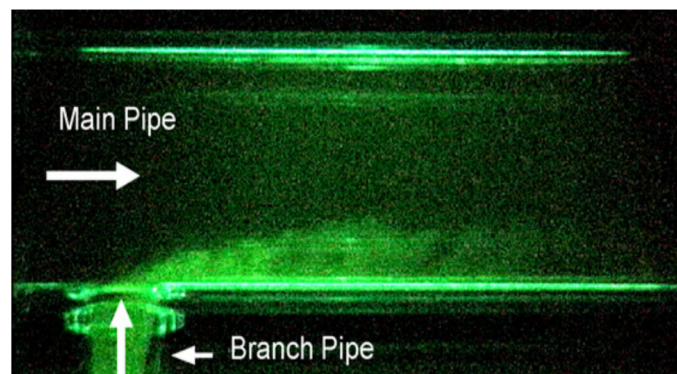


Figure 1: Flow visualization of the 'wall-jet' configuration from [1]

Table 1: Parameters of the WATLON experiment used presently.

Parameters	Main line	Branch line
Mean velocity [m/s]	1.46	0.23
Diameter [mm]	150	50
Bulk Reynolds number	$3,8 \cdot 10^5$	$8,67 \cdot 10^4$
Temperature [°C]	48	33

2 COMPUTATIONAL MODEL

Since the temperature difference is small, the fluid properties can be assumed constant. The incompressible Navier-Stokes equations, accompanied by the thermal energy equation, are solved by using the finite volume-based code OpenFOAM[®]. The system of relevant governing equations reads:

$$\frac{\partial U_i}{\partial x_i} = 0 \quad (1)$$

$$\frac{\partial U_i}{\partial t} + \frac{\partial}{\partial x_j} \left(U_i U_j + \overline{u'_i u'_j} \right) = -\frac{1}{\rho} \frac{\partial P}{\partial x_i} + \frac{\partial}{\partial x_i} \left(\nu \frac{\partial U_i}{\partial x_j} \right) \quad (2)$$

The energy equation is expressed in terms of the temperature evolution equation, yielding:

$$\frac{\partial T}{\partial t} + \frac{\partial}{\partial x_j} \left(U_i T + \overline{u'_i \theta'} \right) = \frac{\partial}{\partial x_i} \left(\alpha \frac{\partial T}{\partial x_j} \right) \quad (3)$$

Subsequently, in order to account for the unresolved turbulence effects, represented through $\overline{u'_i u'_j}$ and $\overline{u'_i \theta'}$, an eddy-resolving turbulence model termed 'Instability-sensitive Reynolds Stress Model' (IS-RSM) has been used [2]. The IS-RSM represents an adequately sensitized URANS model, which is, similar to LES, capable of reproducing the spectral content of turbulence to an appropriate extent, but under the conditions of substantially coarsened spatial and temporal resolutions. Unlike the Smagorinsky-type LES models, the present model accounts for the anisotropy of the residual motion. Modelled portion of the Reynolds stress tensor is accounted for by solving the corresponding evolution equation, which includes the effects of production, redistribution, dissipation, viscous- and turbulent-diffusion as follows:

$$\frac{\partial \overline{u'_i u'_j}}{\partial t} + \frac{\partial}{\partial x_k} \left(U_k \overline{u'_i u'_j} \right) = P_{ij} + \Phi_{ij} - \epsilon_{ij} + D_{ij}^t + D_{ij}^v \quad (4)$$

Further discussion of the Reynolds-Stress model, including also the term-by-term derivation of the viscous dissipation equation, is scrutinized in [3]. The viscous stress dissipation tensor is calculated in terms of its homogeneous part ϵ_{ij}^h :

$$\epsilon_{ij} = \epsilon_{ij}^h + \frac{1}{2} \frac{\partial}{\partial x_k} \left(\nu \frac{\partial \overline{u'_i u'_j}}{\partial x_k} \right) \quad (5)$$

Homogeneous fraction of the total stress dissipation tensor is determined by blending between its wall and off-wall expressions, with the blending function f_s proportional to the turbulence anisotropy:

$$\epsilon_{ij}^h = \epsilon^h \left[(1 - f_s) \frac{2}{3} \delta_{ij} + \frac{\overline{u'_i u'_j}}{k} f_s \right] \quad (6)$$

The specific dissipation rate, representing the inverse of the turbulent time scale, is adopted as the scale-supplying variable:

$$\omega^h = \frac{\varepsilon^h}{k} \quad (7)$$

Furthermore, the additional production term, which shifts the statistical modeling paradigm towards the scale-adaptive framework, is introduced into the ω^h equation (see [3] for its derivation):

$$P_{\Delta U} = 0.003 \max(1.775 \cdot 40 \cdot \kappa \cdot \sqrt{k} \cdot \nabla^2 \mathbf{U} - 40 \cdot T_2, 0) \quad (8)$$

where the term T_2 is introduced to suppress the resolved part of spectrum near the wall:

$$T_2 = 3k \cdot \max\left(\frac{(\omega^h)^2}{(\nabla \omega^h)^2}, \frac{(k)^2}{(\nabla k)^2}\right) \quad (9)$$

Following the presence of the second-derivative of velocity field, non-homogeneities in the shear layer regions (originating e.g. from the flow separation), would trigger additional dissipation of the modelled turbulence fraction, which will consequently shift the major part of the turbulent kinetic energy back to the resolved portion of the spectrum, enabling the emergence of resolved scales. Since the damping of the modelled portion of the spectrum does not explicitly depend on grid spacing, the model will re-adapt the spectral cut-off to the smallest resolvable scale of the mesh. Calibration of model constants is performed in [4] in order to balance modelled and resolved contributions of the spectra. Further optimizations of these constants are possible. Since the model is derived based on the ensemble-averaging technique, native to RANS, it can also return a pure RANS solution, provided that the grid is sufficiently coarse. This 'resolution-on-demand' represents, in line with the high theoretical foundation of the model, an important advantage in comparison with competing LES models.

3 RESULTS AND DISCUSSION

3.1 Precursor simulations

Preliminary investigation on model performance is performed by generating a fully-developed turbulence in both pipes preceding the mixing region in the framework of two precursor simulations. The results obtained are compared to the high Reynolds number pipe measurements by [5], Fig. 2.

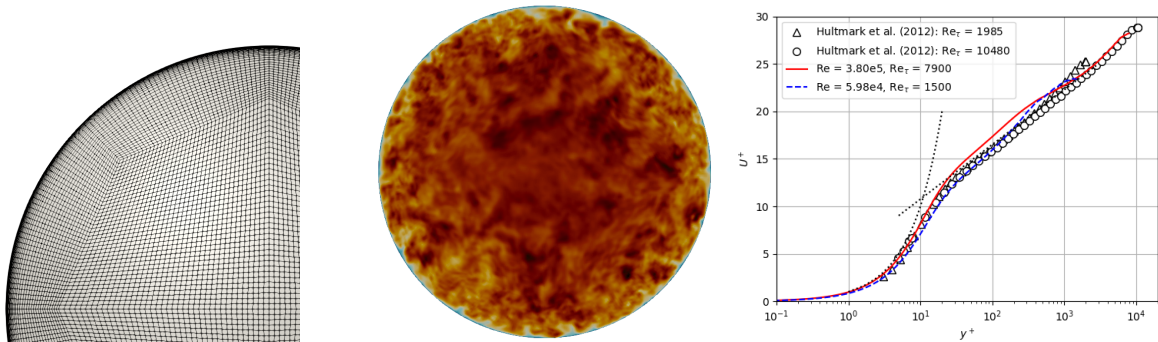


Figure 2: Mesh detail of the precursor pipe flow at $Re = 380,000$ (left), contours of the corresponding instantaneous velocity field (middle), and semi-log plots of the velocity profiles compared to the experimental database from [5]

Good agreement between computations and experiment has been achieved, with deviations less than 4% in the prediction of friction-velocity. It can be seen that the higher Re number case shows somewhat greater deviation from experimental results. The exact reason for this deviation remains open; one

possible remedy would be the re-calibration of model constants to better balance the resolved/modelled portion of the spectrum. Namely, current model is largely calibrated to the range of lower Re numbers corresponding closer to the branch pipe segment, details of which can be found in [4]. Applied meshing strategy represents an optimized trade-off between accuracy and the number of cells. Parameters are provided in Table 2. It can be seen that significant savings can be made by using the IS-RSM model, especially with increase in Reynolds number. Since the overall accuracy proved to be satisfactory, numerical settings and meshing strategy are afterwards beneficially applied in the T-Junction flow configuration.

Table 2: Precursor pipe simulations: mesh parameters.

Parameters	Main line	Branch line
Δr^+	0.5 - 100	0.5 - 100
$\Delta \Theta^+$	100	40
Δz^+	300	120
Mesh size	$\sim 3,600,000$	$\sim 964,000$
Re	$3,8 \cdot 10^5$	$8,67 \cdot 10^4$
Re_τ	7900	2087
ΔU_τ	3.5 %	3.7 %

3.2 Flow and thermal mixing in the T-junction configuration

Starting with the fully developed turbulence from the precursor pipe simulations, the present computational model successfully reproduces the mixing properties involving separation and re-attachment zones as well as secondary flow structures. Following the uneven distribution in momentum, flow coming from the branch pipe is incapable of penetrating further into the main flow and bends instead towards the lower wall of the junction, revealing so the 'wall-jet' type of the flow topology, Fig. 3. The branch stream exhibits a separation at the trailing edge of the junction, creating a flow reversal zone, which is characterized by the low velocity zone above the lower wall. This newly formed separation bubble acts as an obstacle to the mean flow, reducing the effective cross-section, which creates the region of increased axial velocity in the upper portion of the outlet. A small separation zone can also be observed at the leading edge of the T-junction. Despite the turbulent nature of the process, temperature fields show very poor mixing activity in the zone adjacent to the leading edge and the wall-jet boundary, since the main flow doesn't penetrate the separation wake. Large-scale structures, originating from the separation are advected at the wake-edge, enhance the mixing to some extent. This zone of high-energy, low rank structures with high temperature gradients coincides with the wake boundary, and represents a generator of temperature-variance, which is an ideal spot for propagation of the thermally induced fatigue.

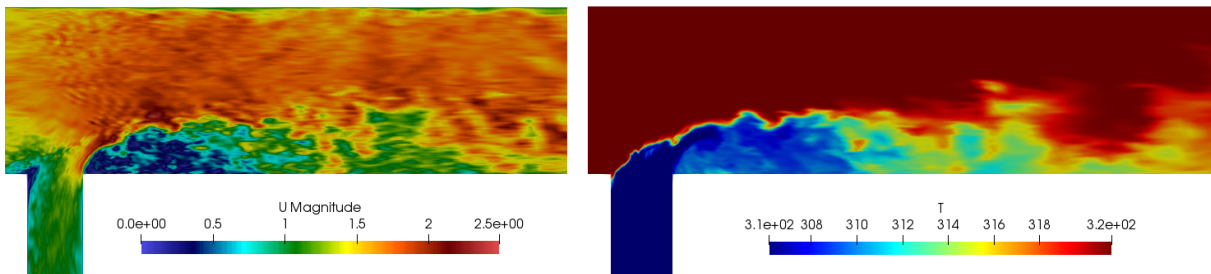


Figure 3: Contours of the instantaneous velocity (right) and temperature fields (left).

Numerical mesh, including precursor pipes, comprises approx. 18 Million cells in total, which is a significant computational saving in comparison to similar cases. Exemplary, Tunstall [6] reported an LES T-junction study at comparable Reynolds number, with overall meshing size of ~ 80 Million cells. The comparison between experimental and calculated mean streamline patterns reveals very good agreement. The position of the mean-dividing streamline, as well as the zeroth velocity line have been accurately captured. Both the shape and the dimensions of the separation bubble are in close agreement with those experimentally determined, with the size corresponding to $\sim 2D_m$. Secondary separation bubble, in the vicinity of the mean-dividing line, could not be clearly recovered in the present numerical study.

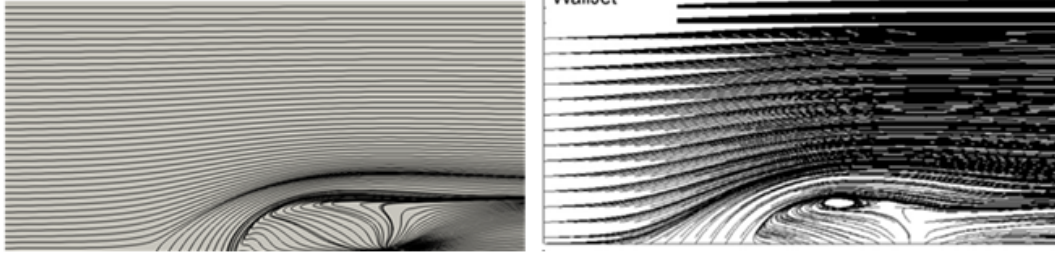


Figure 4: Streamlines of the mean velocity field: simulation (right) and experiment (left).

Direct comparison of the mean axial velocity and temperature profiles and corresponding root-mean-square components evaluated at the position just inside the separation zone shows a good agreement between experiment and calculations (Fig. 5), indicating a sufficiently-well resolved turbulent spectrum in this complex flow configuration. An additional interpretation of results can be made from the viewpoint of temporal dynamics. Fig. 6 displays instantaneous temperature field at the bottom wall. Behind the mixing zone, the characteristic street of switching vortical structures develops, exposing the wall to the periodically changing temperature field, which leads to the emergence of thermally induced stresses.

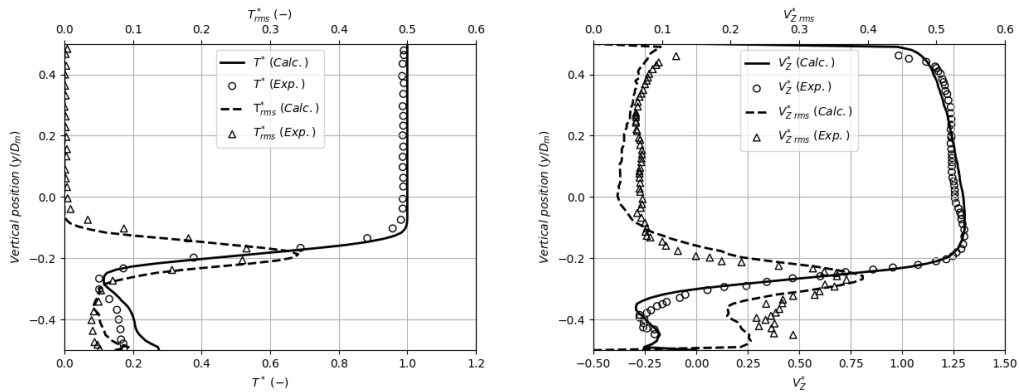


Figure 5: Mean temperature (left) and axial velocity profiles (right) and corresponding root-mean-square quantities at the location $0.5 D_m$ downstream of the junction center, positioned directly inside the separation zone.

Spectral characteristics of such structures are further investigated by using the FFT Analysis, and by Welch spectral estimator in order to reduce frequency scatterings. Measuring probe is positioned inside the wake with coordinates $(0.035, 0.065, 0.075)$. Origin is placed at the intersection of pipe axis. Frequency peaks are pronounced between 4 and 6 Hz, which corresponds very well to the theoretical range shedding frequency reported by [1], Fig. 7. The obtained frequency signature also shows a theoretically correct slope of $-5/3$, indicating directly the correctly resolved turbulence spectrum by using the present turbulence model.

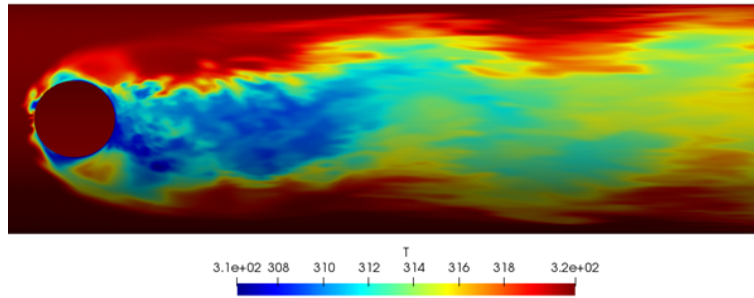


Figure 6: Contours of instantaneous temperature field at the bottom wall.

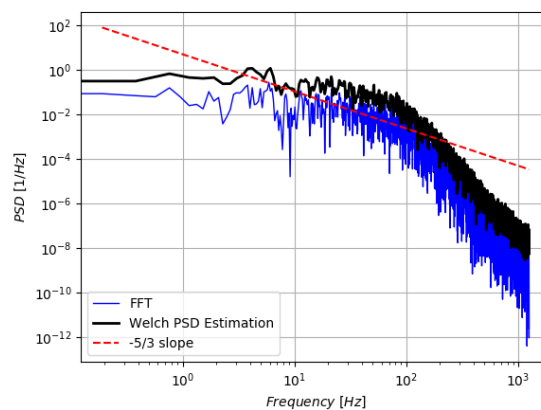


Figure 7: Frequency signature of the temperature field inside the wake with accompanying Welch PSD estimation.

4 CONCLUSIONS

The predictive performance of a RANS-based eddy-resolving strategy, based on a Reynolds stress model formulation functioning as a sub-scale model, has been validated by simulating a high Reynolds number case involving the mixing of two fluid streams at different temperatures in a T-junction geometry. Comparison with experimental data shows that the applied turbulence model, complemented by an appropriate numerical algorithm and mesh resolution, provides a reliable computational framework for simulating complex turbulence phenomena relevant to the NPP industry, with significant computation cost savings due to the coarser mesh resolution usually required for standard LES calculations.

REFERENCES

- [1] I. M. K. S. K. N. Kamide, H. & K. Hayashi. Study on mixing behavior in a tee piping and numerical analyses for evaluation of thermal striping. *Nuclear Engineering and Design*, **239** (2009) 58–67.
- [2] S. Jakirlic & R. Maduta. Extending the bounds of ‘steady’ RANS closures: Toward an instability-sensitive Reynolds stress model. *International Journal of Heat and Fluid Flow*, **51** (2015) 175–194.
- [3] S. Jakirlic & K. Hanjalic. A new approach to modelling near-wall turbulence energy and stress dissipation. *Journal of Fluid Mechanics*, **459** (2002) 139–166.
- [4] R. Maduta. *An eddy-resolving Reynolds stress model for unsteady flow computations: development and application*. Ph.D. thesis, Technische Universität Darmstadt, Darmstadt, Germany (2013).
- [5] V. M. B. S. C. C. Hultmark, M. & A. J. Smits. Turbulent Pipe Flow at Extreme Reynolds Numbers. *Physical Review Letters*, **108**.
- [6] R. Tunstall, D. Laurence, R. Prosser, & A. Skillen. Large eddy simulation of a T-Junction with upstream elbow: The role of Dean vortices in thermal fatigue. *Applied Thermal Engineering*, **107** (2016) 672–680.